DESIGN OF ACTIVE INDUCTOR AND STABILITY TEST FOR PASSIVE RLC LOW-PASS FILTER

MinhTri Tran, Anna Kuwana, and Haruo Kobayashi

Division of Electronics and Informatics,
Gunma University, Kiryu 376-8515, Japan

ABSTRACT

Proposed stability test for RLC low-pass filters is presented. The self-loop functions of these filters are derived and analyzed based on the widened superposition principle. The alternating current conservation technique is proposed to measure the self-loop function. An active inductor is replaced with a general impedance converter. Our research results show that the values of the selected passive components (resistors, capacitors, and inductors) in these filters can cause a damped oscillation noise when the stable conditions for the transfer functions of these networks are not satisfied.

KEYWORDS

Widened Superposition, RLC Low-Pass Filter, Stability Test, Self-loop Function, Voltage Injection.

1. INTRODUCTION

Analogue filters are essential in removing noise signals that may accompany a desired signal [1]. Passive low-pass filters employ RLC circuits, but they become impractical at very low frequencies because of large physical size of inductors and capacitors [2]. Moreover, feedback control theories are widely applied in the processing of analogue signals [3]. In conventional analysis of a feedback system, the term of "$A\beta(s)$" is called loop gain when the denominator of a transfer function is simplified as $1+A\beta(s)$, where $A(s)$, $\beta(s)$, are the open loop gain, and the feedback gain, respectively. The stability of a feedback network is determined by the magnitude and phase plots of the loop gain. However, the passive filter is not a closed loop system. Furthermore, the denominator of the transfer function of the analogue filter, regardless of active or passive is also simplified as $1+L(s)$, where $L(s)$ is called "self-loop function". Therefore, the term of "self-loop function" is proposed to define $L(s)$ for both cases with and without feedback filters. This paper provides an introduction to the derivation of the transfer function, the measurement of the self-loop function and the stability test for RLC low-pass filters.

The main contribution of this paper comes from the stability test for the RLC low-pass filters based on the widened superposition principle and the alternating current conservation measurement. This paper contains a total of 8 sections and 2 appendices. Section 2 constitutes background knowledge, with an explanation of the necessity for network analysis based on the widened superposition principle, an essence of derivation of self-loop function based on an alternating current conversation measurement and a brief presentation of the complex function. Section 3 mathematically analyzes an illustrative second-order denominator complex function

David C. Wyld et al. (Eds): CCSEA, BIoT, DKMP, CLOUD, NLCAI, SIPRO - 2020
pp. 203-224, 2020. CS & IT - CSCP 2020 DOI: 10.5121/csit.2020.101016

considered in details. Section 4 and Section 5 focus on the frequency domain analysis and the stability test for serial and parallel RLC low-pass filters. SPICE simulation results for the proposed design of active inductors for the RLC low pass filters are described in Section 6. A brief discussion of the research results is given in Section 7. The main points of this work are summarized in Section 8. We have collected a few important notions and results from analysis in Appendix for easy references.

2. DESIGN CONSIDERATIONS FOR RLC LOW-PASS FILTER

2.1. Widened Superposition Principle

In this section, we propose a new concept of the superposition principle which is useful for deriving the transfer function of a network. The conventional superposition theorem is used to find the solution to linear networks consisting of two or more sources (independent sources, linear dependent sources) that are not in series or parallel. To consider the effects of each source independently requires that sources be removed and replaced without affecting the final result. Therefore, to remove a voltage source when applying this theorem, the difference in potential between the terminals of the voltage source must be set to zero (short circuit); removing a current source requires that its terminals be opened (open circuit). This procedure is followed for each source in turn, and then the resultant responses are added to determine the true operation of the circuit. There are some limitations of conventional superposition theorem. Superposition cannot be applied to power effects because the power is related to the square of the voltage across a resistor or the current through a resistor. Superposition theorem cannot be applied for non-linear circuit (diodes or transistors). In order to calculate the load current or the load voltage for the several choices of the load resistance of the resistive network, one needs to solve for every source voltage and current, perhaps several times. With the simple circuit, this is fairly easy but in a large circuit this method becomes a painful experience.

In this paper, the nodal analysis on circuits is used to obtain multiple Kirchhoff current law equations. The term of "widened superposition" is proposed to define a general superposition principle which is the standard nodal analysis equation, and simplified for the case when the impedance from node A to ground is infinity and the current injection into node A is 0. In a circuit having more than one independent source, we can consider the effects of all the sources at a time. The widened superposition principle is used to derive the transfer function of a network [4, 5]. Energy at one place is proportional with their input sources and the resistance distances of transmission spaces. Let $E_A(t)$ be energy at one place of multi-sources $E_i(t)$ which are transmitted on the different resistance distances d_i (R, Z_L, and Z_C in electronic circuits) of the transmission spaces as shown in Figure 1. The widened superposition principle is defined as

$$E_A(t)\sum_{i=1}^{n}\frac{1}{d_i} = \sum_{i=1}^{n}\frac{E_i(t)}{d_i} \tag{1}$$

The import of these concepts into circuit theory is relatively new with much recent progress regarding filter theory, analysis and implementation.

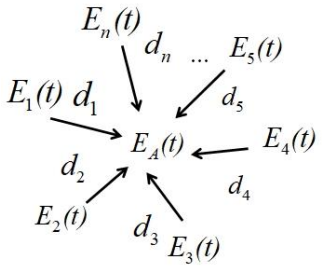

Figure 1. Energy at one node based on superposition principle

2.2. Complex Function

In this section, we describe a transfer function as the form of a complex function where the variable is an angular frequency. In frequency domain, the transfer function and the self-loop function of a filter are complex functions. Complex functions are typically represented in two forms: polar or rectangular. The polar form and the rectangular representation of a complex function H(jω) is written as

$$H(j\omega) = \mathrm{Re}\{H(j\omega)\} + j\,\mathrm{Im}\{H(j\omega)\} = \sqrt{\left(\mathrm{Re}\{H(j\omega)\}\right)^2 + \left(\mathrm{Im}\{H(j\omega)\}\right)^2}\, e^{j\arctan\left(\frac{\mathrm{Im}\{H(j\omega)\}}{\mathrm{Re}\{H(j\omega)\}}\right)} \qquad (2)$$

where Re{H(jω)} is the real part of H(jω) and Im{H(jω)} is the imaginary part of H(jω), and j is the imaginary operator $j^2 = -1$. The real quantity $\sqrt{\left(\mathrm{Re}\{H(j\omega)\}\right)^2 + \left(\mathrm{Im}\{H(j\omega)\}\right)^2}$ is known as the amplitude or magnitude, the real quantity $\arctan\left(\frac{\mathrm{Im}\{H(j\omega)\}}{\mathrm{Re}\{H(j\omega)\}}\right)$ is called the angle $\angle H(j\omega)$, which is the angle between the real axis and $H(j\omega)$. The angle may be expressed in either radians or degrees and real quantity $\frac{\mathrm{Im}\{H(j\omega)\}}{\mathrm{Re}\{H(j\omega)\}}$ is called the argument $Arg\{H(j\omega)\}$ which is the ratio between the real part and the imaginary part of H(jω). The operations of addition, subtraction, multiplication, and division are applied to complex functions in the same manner as that they are to complex numbers. Complex functions are typically expressed in three forms: magnitude-angular plots (Bode plots), polar charts (Nyquist charts), and magnitude-argument diagrams (Nichols diagrams). In this paper, the stability test is performed on the magnitude-angular plots and the polar charts of the self-loop function.

2.3. Graph Signal Model for Complex Function

In this section, we describe the graph signal model of a typical complex function which is the same as the graph signal model of a feedback system. A negative-feedback amplifier is an electronic amplifier that subtracts a fraction of its output from its input, so that negative feedback opposes the original signal. The applied negative feedback can improve its performance (gain stability, linearity, frequency response, step response) and reduce sensitivity to parameter variations due to manufacturing or environment. Thanks to these advantages, many amplifiers and control systems use negative feedback. However, the denominator complex functions are also expressed in the graph signal model which is the same as the negative feedback system. A general denominator complex function is rewritten as

$$H(s) = \frac{V_{out}(s)}{V_{in}(s)} = \frac{A(s)}{1 + L(s)} \tag{3}$$

This form is called the standard form of the denominator complex function. The output signal is calculated as

$$V_{out}(s) = A(s)\left[V_{in}(s) - \frac{L(s)}{A(s)} V_{out}(s) \right] \tag{4}$$

Figure 2 presents the graph signal model of a general denominator complex function. The feedback system is unstable if the closed-loop "gain" goes to infinity, and the circuit can amplify its own oscillation. The condition for oscillation is

$$L(s) = -1 = 1e^{-j\pi(2k+1)}; k \in Z \tag{5}$$

Through the self-loop function, a second-order denominator complex function can be found that is stable or not. The concepts of phase margin and gain margin are used to asset the characteristics of the loop function at unity gain in magnitude-phase plots (Bode plots) [6].

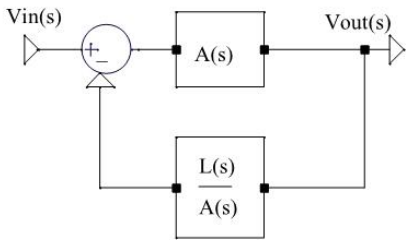

Figure 2. Graph signal model of general complex function.

2.4. Alternating Current Conservation Measurement

This section describes a mathematical way to measure the self-loop function based on the alternating current conservation when we inject alternating signal sources (alternating current or voltage sources) and connect the input of the network into the alternating current ground (AC ground). In general, the term of "alternating current conservation" is proposed to define this technique. The main idea of this method is that the alternating current is conserved. In other words, at the output node the incident alternating current is equal to the transmitted alternating current. If we inject an alternating current source (or an alternating voltage source) at the output node, the self-loop function can be derived by ratio of the incident voltage (V_{inc}) and the transmitted voltage (V_{tran}) as shown in Figures 3(a), 3(c), and 3(d). Compared to measurement results of the alternating current conservation with the conventional ones (voltage injection), they are the same [7]. Apply the widened superposition principle at V_{inc} and V_{tran} nodes, and the self-loop function is derived as

$$\frac{V_{inc}}{A(s)} = -\frac{L(s)}{A(s)} V_{tran} \Rightarrow L(s) = -\frac{V_{inc}}{V_{tran}} \tag{6}$$

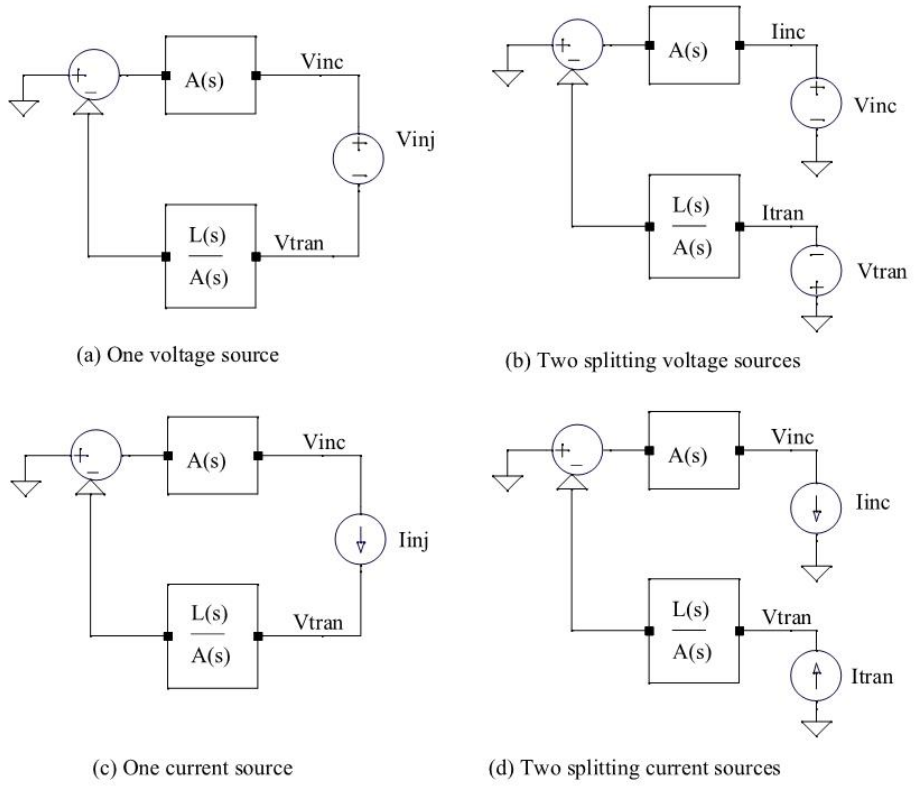

Figure 3. Derivation of self-loop function based on alternating current conservation.

In case of Figure 3(b), the alternating currents are used to derive the self-loop function. Apply the widened superposition principle at I_{inc} and I_{tran} nodes, and the self-loop function is derived as

$$I_{inc}A(s) = \frac{A(s)}{L(s)} I_{tran} \Rightarrow L(s) = \frac{I_{tran}}{I_{inc}} \tag{7}$$

3. ANALYSIS OF SECOND-ORDER DENOMINATOR COMPLEX FUNCTION

3.1. Second-Order Denominator Complex Function

In this section, we shall analyze the frequency response of a typical second-order denominator complex function. This complex function is defined as in Equation (8). Assume that all constant variables are not equal to zero.

$$H(s) = \frac{1}{as^2 + bs + c} \tag{8}$$

From Equation (27) in Appendix A.1, the simplified complex function is written as

$$H(j\omega) = \frac{\frac{4a}{b^2}}{\left(1 + j\frac{2a}{b}\omega\right)^2 + \left(\frac{2a}{b}\right)^2 \left[\frac{c}{a} - \left(\frac{b}{2a}\right)^2\right]} \tag{9}$$

In order to plot the magnitude-angular charts, the values of magnitude-angular of the complex function, which are calculated in Appendix A.1, are summarized on Table 1. In overdamped case, the magnitude of the complex function is so high from the first cut-off angular frequency $\omega_{cut1} = \left| \frac{b}{2a}\left(1 - \frac{2a}{b}\sqrt{\frac{c}{a} - \left(\frac{b}{2a}\right)^2}\right)\right|$ to the second cut-off angular frequency $\omega_{cut2} = \left| \frac{b}{2a}\left(1 - \frac{2a}{b}\sqrt{\frac{c}{a} - \left(\frac{b}{2a}\right)^2}\right)\right|$. Therefore, this gain will amplify the high order harmonics from ω_{cut1} to ω_{cut2} of an input signal which includes many harmonics.

3.2. Damped Oscillation Noise

In this section, we describe the response of a typical second-order denominator complex function to a step input or a square wave. Based on the Fourier series expansion of the square wave, the waveforms of the pulse wave are expressed in many functions of time with many different frequencies as shown in Figure 7. The waveform function of a square wave is

$$S(t) = \frac{4}{\pi}\sum_{k=1}^{\infty}\frac{\sin\left(2\pi(2k-1)(f_1)t\right)}{2k-1} \tag{10}$$

- In under-damped case, the high-order harmonics of the step signal are significantly reduced from the first cut-off angular frequency. Therefore, the rising time and falling time are rather short. In this case, the system is absolutely stable.
- In critically damped case, the rising time and falling time are longer than the underdamped case. Now, the system is marginally stable. The energy propagation is also maximal because this condition is equal to the balanced charge-discharge time condition [8].
- In over-damped case, the gain at the cut-off angular frequency will amplify the high-order harmonics of the step signal that causes the peaking or ringing. Ringing is an unwanted oscillation of a voltage or current.

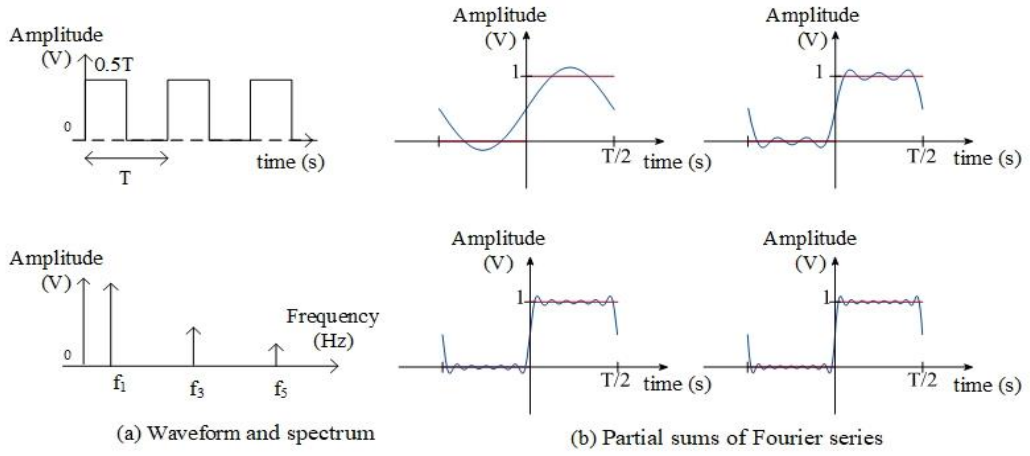

Figure 4. Waveform, spectrum, and partial sums of Fourier series of square wave.

The term of "damped oscillation noise" is proposed to define this unwanted oscillation which fades away with time, particularly in the step response (the response to a sudden change in input). Damped oscillation noise is undesirable because it causes extra current to flow, which leads to thereby wasting energy and causing extra heating of the components. It can cause unwanted electromagnetic radiation to be emitted. Therefore, the system is unstable.

3.3. Self-Loop Function of Second-Order Denominator Complex Function

In this section, we investigate the characteristics of the self-loop function L(s). The general second-order denominator complex function and its self-loop function are rewritten as in Equation (11). The magnitude-angular values and the real-imagine values of the self-loop function, which are calculated in Appendix A.2, are summarized in Table 2. In this work, the self-loop function is sketched on the magnitude-angular plots and polar charts.

$$H(j\omega)=\frac{\frac{4a}{b^2}}{1+\left(\frac{2a}{b}\right)^2(j\omega)^2+2\left(\frac{2a}{b}\right)j\omega+\left(\frac{2a}{b}\right)^2\left[\frac{c}{a}-\left(\frac{b}{2a}\right)^2\right]};\ L(j\omega)=j\frac{4a}{b}\omega-\left(\frac{2a}{b}\omega\right)^2+\left(\frac{2a}{b}\right)^2\left[\frac{c}{a}-\left(\frac{b}{2a}\right)^2\right] \tag{11}$$

4. STABILITY TEST FOR SERIAL RLC LOW-PASS FILTER

4.1. Analysis of Serial RLC Low-Pass Filter

In this section, we shall present the frequency response of a serial RLC low-pass filter. Models of circuit and measurement of self-loop function for this filter are shown in Figure 5. Apply the widened superposition at output node on Figure 5(a), we get

$$V_{out}\left(\frac{1}{R+Z_L}+\frac{1}{Z_C}\right)=\frac{V_{in}}{R+Z_L} \tag{12}$$

The transfer function and the self-loop function are derived as

$$H(s)=\frac{V_{out}}{V_{in}}=\frac{1}{1+\frac{R+Z_L}{Z_C}}=\frac{1}{1+sC\left(R+sL\right)};\ L(s)=LCs^2+sRC \tag{13}$$

Table 1. Summary of magnitude-angular values of transfer function

Case	Underdamped		Critically damped		Overdamped	
Delta (Δ)	$\frac{c}{a}<\left(\frac{b}{2a}\right)^2\Rightarrow\Delta=b^2-4ac>0$		$\frac{c}{a}=\left(\frac{b}{2a}\right)^2\Rightarrow\Delta=b^2-4ac=0$		$\frac{c}{a}>\left(\frac{b}{2a}\right)^2\Rightarrow\Delta=b^2-4ac<0$	
Module $\lvert H(\omega)\rvert$	$\frac{\frac{4a}{b^2}}{\sqrt{\left(\frac{4a}{b}\omega\right)^2+\left(1-\left(\frac{2a}{b}\omega\right)^2-\left\lvert\left(\frac{2a}{b}\right)^2\left[\frac{c}{a}-\left(\frac{b}{2a}\right)^2\right]\right\rvert\right)^2}}$		$\frac{\frac{4a}{b^2}}{\sqrt{\left(\frac{4a}{b}\omega\right)^2+\left(1-\left(\frac{2a}{b}\omega\right)^2\right)^2}}$		$\frac{\frac{4a}{b^2}}{\sqrt{\left(\frac{4a}{b}\omega\right)^2+\left(1-\left(\frac{2a}{b}\omega\right)^2+\left\lvert\left(\frac{2a}{b}\right)^2\left[\frac{c}{a}-\left(\frac{b}{2a}\right)^2\right]\right\rvert\right)^2}}$	
Angular $\angle H(\omega)$	$\arctan\left(\frac{-\frac{4a}{b}\omega}{1-\left(\frac{2a}{b}\omega\right)^2-\left\lvert\left(\frac{2a}{b}\right)^2\left[\frac{c}{a}-\left(\frac{b}{2a}\right)^2\right]\right\rvert}\right)$		$\arctan\left(\frac{-\frac{4a}{b}\omega}{1-\left(\frac{2a}{b}\omega\right)^2}\right)$		$\arctan\left(\frac{-\frac{4a}{b}\omega}{1-\left(\frac{2a}{b}\omega\right)^2+\left\lvert\left(\frac{2a}{b}\right)^2\left[\frac{c}{a}-\left(\frac{b}{2a}\right)^2\right]\right\rvert}\right)$	
$\omega=\frac{b}{2a}$	$\lvert H(\omega)\rvert<\frac{1}{2}\frac{4a}{b^2}$	$\angle H(\omega)>-\frac{\pi}{2}$	$\lvert H(\omega)\rvert=\frac{1}{2}\frac{4a}{b^2}$	$\angle H(\omega)=-\frac{\pi}{2}$	$\lvert H(\omega)\rvert>\frac{1}{2}\frac{4a}{b^2}$	$\angle H(\omega)<-\frac{\pi}{2}$

Table 2. Summary of magnitude-angular values and real-imagine values of self-loop function

Case	Underdamped		Critically damped		Overdamped	
Delta (Δ)	$\Delta = b^2 - 4ac > 0$		$\Delta = b^2 - 4ac = 0$		$\Delta = b^2 - 4ac < 0$	
$\lvert L(j\omega)\rvert$	$\sqrt{\left(\frac{4a}{b}\omega\right)^2 + \left(\left\lvert\left(\frac{2a}{b}\right)^2\left[\frac{c}{a} - \left(\frac{b}{2a}\right)^2\right]\right\rvert - \left(\frac{2a}{b}\omega\right)^2\right)^2}$		$\sqrt{\left(\frac{4a}{b}\omega\right)^2 + \left(\frac{2a}{b}\omega\right)^4}$		$\sqrt{\left(\frac{4a}{b}\omega\right)^2 + \left(-\left\lvert\left(\frac{2a}{b}\right)^2\left[\frac{c}{a} - \left(\frac{b}{2a}\right)^2\right]\right\rvert - \left(\frac{2a}{b}\omega\right)^2\right)^2}$	
$\angle L(j\omega)$	$\arctan\left(\frac{\frac{4a}{b}\omega}{\left\lvert\left(\frac{2a}{b}\right)^2\left[\frac{c}{a} - \left(\frac{b}{2a}\right)^2\right]\right\rvert - \left(\frac{2a}{b}\omega\right)^2}\right)$		$\arctan\left(-\frac{2}{\left(\frac{2a}{b}\omega\right)}\right)$		$\arctan\left(\frac{\frac{4a}{b}\omega}{-\left\lvert\left(\frac{2a}{b}\right)^2\left[\frac{c}{a} - \left(\frac{b}{2a}\right)^2\right]\right\rvert - \left(\frac{2a}{b}\omega\right)^2}\right)$	
$\omega = \frac{b}{2a}\sqrt{\sqrt{5}-2}$	$\lvert L(\omega)\rvert > 1$	$\angle L(\omega) < -76.3^o$	$\lvert L(\omega)\rvert = 1$	$\angle L(\omega) = -76.3^o$	$\lvert L(\omega)\rvert < 1$	$\angle L(\omega) > -76.3^o$
$\omega = \frac{b}{2a}$	$\lvert L(\omega)\rvert > \sqrt{5}$	$\angle L(\omega) < -63.4^o$	$\lvert L(\omega)\rvert = \sqrt{5}$	$\angle L(\omega) = -63.4^o$	$\lvert L(\omega)\rvert < \sqrt{5}$	$\angle L(\omega) > -63.4^o$
$\omega = \frac{b}{a}$	$\lvert L(\omega)\rvert > 4\sqrt{2}$	$\angle L(\omega) < -45^o$	$\lvert L(\omega)\rvert = 4\sqrt{2}$	$\angle L(\omega) = -45^o$	$\lvert L(\omega)\rvert < 4\sqrt{2}$	$\angle L(\omega) > -45^o$
$\mathrm{Re}\{L(j\omega)\}$	$-\left(\frac{2a}{b}\omega\right)^2 + \left\lvert\left(\frac{2a}{b}\right)^2\left[\frac{c}{a} - \left(\frac{b}{2a}\right)^2\right]\right\rvert$		$-\left(\frac{2a}{b}\omega\right)^2$		$-\left(\frac{2a}{b}\omega\right)^2 - \left\lvert\left(\frac{2a}{b}\right)^2\left[\frac{c}{a} - \left(\frac{b}{2a}\right)^2\right]\right\rvert$	
$\mathrm{Im}\{L(j\omega)\}$	$\frac{4a}{b}\omega$		$\frac{4a}{b}\omega$		$\frac{4a}{b}\omega$	
$\omega = \frac{b}{2a}\sqrt{\sqrt{5}-2}$	$\mathrm{Re} < 2 - \sqrt{5}$	$\mathrm{Im} = 2\sqrt{\sqrt{5}-2}$	$\mathrm{Re} = 2 - \sqrt{5}$	$\mathrm{Im} = 2\sqrt{\sqrt{5}-2}$	$\mathrm{Re} > 2 - \sqrt{5}$	$\mathrm{Im} = 2\sqrt{\sqrt{5}-2}$
$\omega = \frac{b}{2a}$	$\mathrm{Re} < -1$	$\mathrm{Im} = 2$	$\mathrm{Re} = -1$	$\mathrm{Im} = 2$	$\mathrm{Re} > -1$	$\mathrm{Im} = 2$
$\omega = \frac{b}{a}$	$\mathrm{Re} < -4$	$\mathrm{Im} = 4$	$\mathrm{Re} = -4$	$\mathrm{Im} = 4$	$\mathrm{Re} > -4$	$\mathrm{Im} = 4$

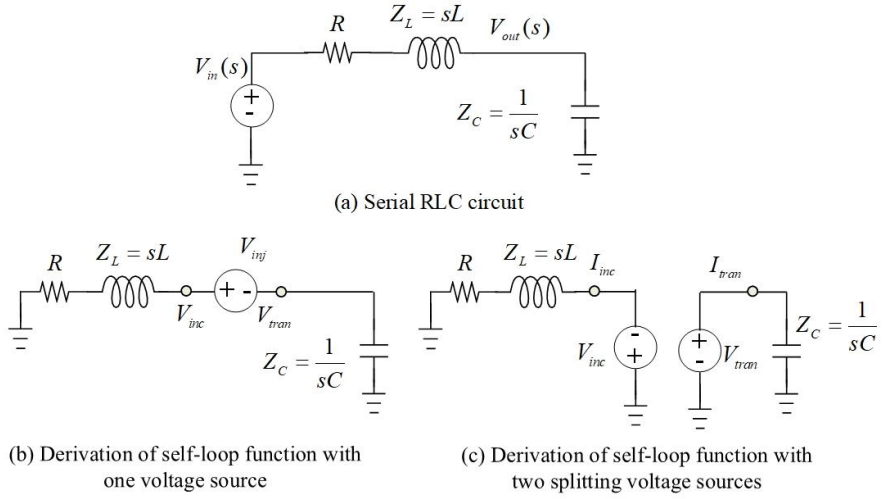

Figure 5. Models of circuit and measurement of self-loop function for serial RLC LPF.

The simplified form of transfer function is

$$H(s)=\frac{\frac{4L}{R^2C}}{\left(\frac{2L}{R}s+1\right)^2+\left(\frac{2L}{R}\right)^2\left[\frac{1}{LC}-\left(\frac{R}{2L}\right)^2\right]} \tag{14}$$

Here, the resonant and the cut-off angular frequencies are $\omega_{LC}=\frac{1}{\sqrt{\mathrm{LC}}}$; $\omega_{RL}=\frac{R}{2L}$. The constraints of the stability for a serial RLC low-pass filter are defined as

$$\frac{1}{LC}>\left(\frac{R}{2L}\right)^2 \Rightarrow \quad |Z_L|=|Z_C|>\frac{R}{2} \quad ; \quad \text{(Instability)} \tag{15}$$

$$\frac{1}{LC}=\left(\frac{R}{2L}\right)^2 \Rightarrow \quad |Z_L|=|Z_C|=R/2 \quad ; \quad \text{(Marginal stability)} \tag{16}$$

$$\frac{1}{LC}<\left(\frac{R}{2L}\right)^2 \Rightarrow \quad |Z_L|=|Z_C|<\frac{R}{2} \quad ; \quad \text{(Stability)} \tag{17}$$

4.2. Stability Test for Serial RLC Low-Pass Filter

This section will present a stability test for a serial RLC low-pass filter. Three models of this filter are used to do the damped oscillation noise test. The marginally stable model is designed at cut-off frequency f_0 = 50 kHz taking L = 796 μH, C = 3.18 nF, and R = 1 kΩ based on a balanced charge and discharge time condition as shown in Figure 6(b). Figures 6(a) and 6(c) are unconditionally stable (R = 1.5 kΩ), and unstable (R = 0.5 kΩ), respectively. Figures 6(e), 6(d) and 6(f) are the measurements of these self-loop functions with one voltage source. Moreover, two splitting voltage sources are also used to measure the self-loop functions as shown in Figures 6(g), 6(h) and 6(i). Figure 7(a) represents the SPICE simulation results of the magnitude of the serial RLC circuit on the frequency domain. In time domain, when the pulse signals go in to these models, the transient responses are shown in Figure 7(b). Figures 7(c), 7(d), 7(e), 7(f), 7(g), 7(h), and 7(i) show the simulation results of the self-loop function on the magnitude-angular plots and polar charts.

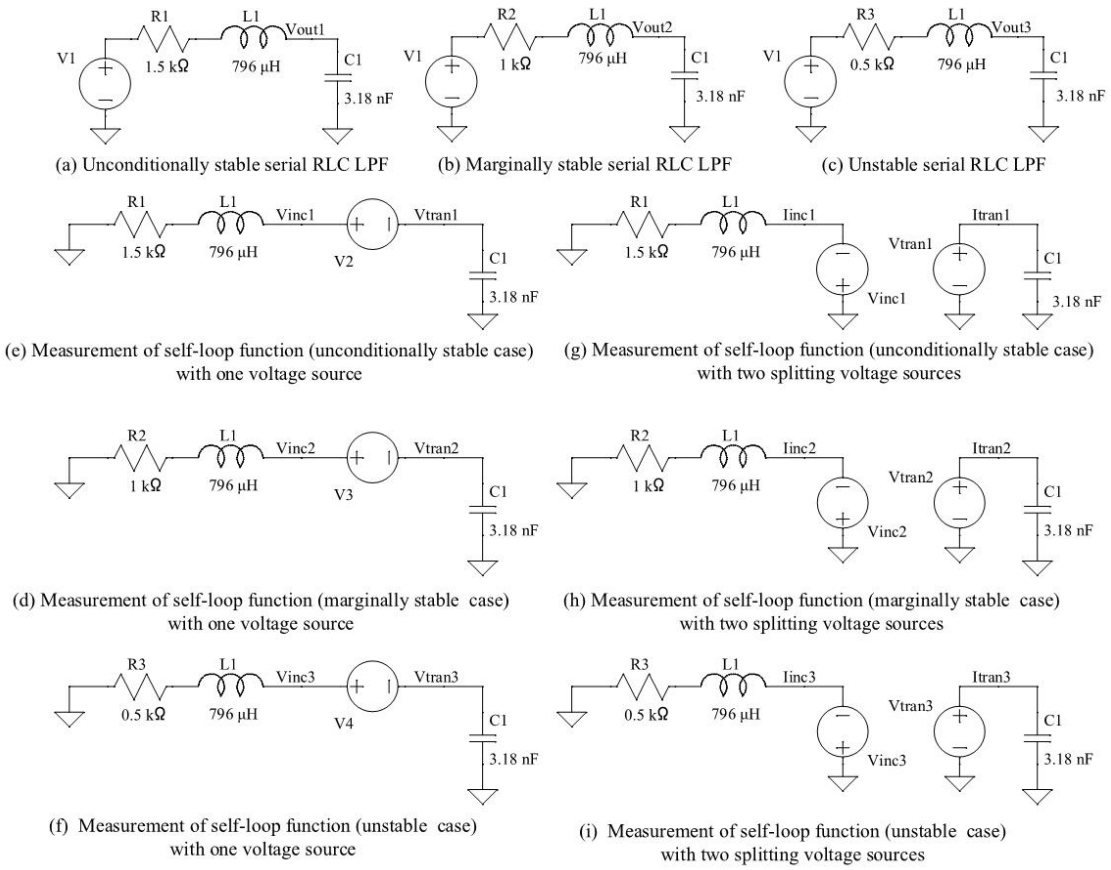

Figure 6. Models of circuits and measurements of self-loop functions for RLC low-pass filter.

The simulation results of the frequency responses of transfer functions and self-loop functions are the same as the characteristics on Table 1 and Table 2. The damped oscillation noise (red) occurs in case of the unstable serial RLC circuit. In theoretical calculation at the cut-off frequency 50 kHz is 76.3 degrees. Our simulation results of self-loop functions show that

- In stable case, phase is 95.7 degrees at 50 kHz, (phase margin = 84.3 degrees).
- In marginally stable case, phase is 104 degrees at 50 kHz, (phase margin = 76 degrees).
- In unstable case, phase margin is 116 degrees at 50kHz, (phase margin = 64 degrees).

The simulation results and the values of theoretical calculation are unique.

5. STABILITY TEST FOR PARALLEL RLC LOW-PASS FILTER

5.1. Analysis of Parallel RLC Low-Pass Filter

In this section, we shall present the frequency response of a parallel RLC low-pass filter. Models of circuit and measurement of self-loop function for this filter are shown in Figure 8. Apply the widened superposition at output node

$$V_{out}\left(\frac{1}{R}+\frac{1}{Z_C}+\frac{1}{Z_L}\right)=\frac{V_{in}}{Z_L} \tag{18}$$

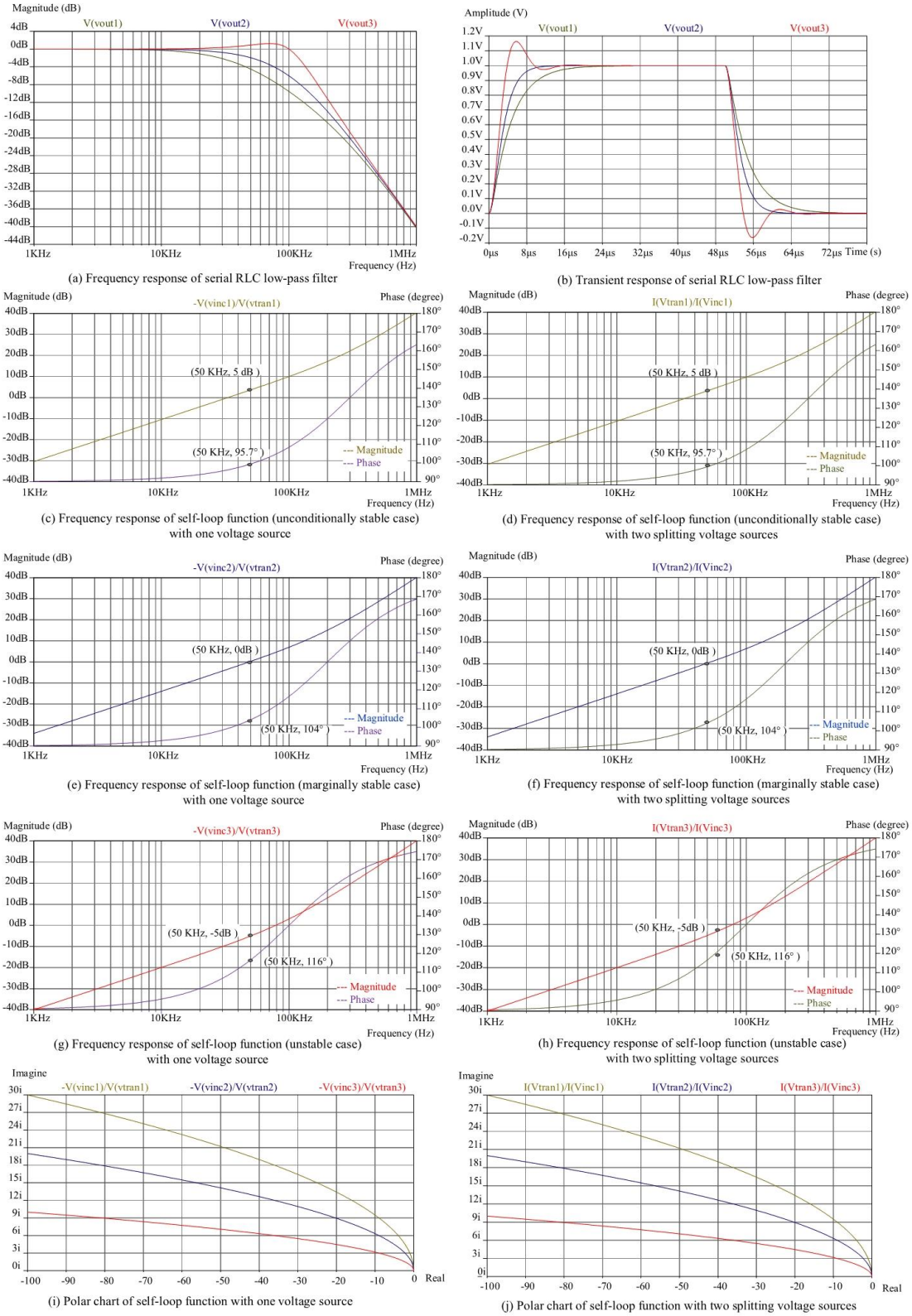

(a) Frequency response of serial RLC low-pass filter

(b) Transient response of serial RLC low-pass filter

(c) Frequency response of self-loop function (unconditionally stable case) with one voltage source

(d) Frequency response of self-loop function (unconditionally stable case) with two splitting voltage sources

(e) Frequency response of self-loop function (marginally stable case) with one voltage source

(f) Frequency response of self-loop function (marginally stable case) with two splitting voltage sources

(g) Frequency response of self-loop function (unstable case) with one voltage source

(h) Frequency response of self-loop function (unstable case) with two splitting voltage sources

(i) Polar chart of self-loop function with one voltage source

(j) Polar chart of self-loop function with two splitting voltage sources

Figure 7. Frequency response, transient response, polar charts and magnitude-phase plots of self-loop function for serial RLC low-pass filter.

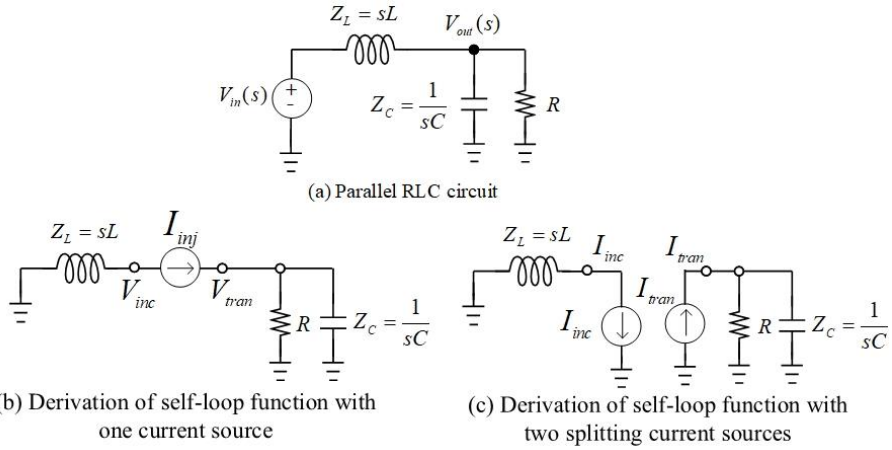

Figure 8. Models of circuit and measurement of self-loop function for parallel RLC LPF.

Then, the transfer function and the self-loop function of the parallel RLC low-pass filter are

$$H(s) = \frac{V_{out}}{V_{in}} = \frac{1}{1 + Z_L\left(\frac{1}{R} + \frac{1}{Z_C}\right)} = \frac{1}{LCs^2 + s\frac{L}{R} + 1}; \; L(s) = LCs^2 + s\frac{L}{R} \tag{19}$$

The simplified form of Equation (19) is

$$H(s) = \frac{\frac{4R^2C}{L}}{(2RCs+1)^2 + (2RC)^2\left[\frac{1}{LC} - \left(\frac{1}{2RC}\right)^2\right]} \tag{20}$$

Here, the resonant and the cut-off angular frequencies are $\omega_{LC} = \frac{1}{\sqrt{\mathrm{LC}}}; \; \omega_{RC} = \frac{1}{2RC}$. The constraints of the stability for the parallel RLC low-pass filter are defined as

$$\frac{1}{LC} > \left(\frac{1}{2RC}\right)^2 \quad \Rightarrow \quad |Z_L| = |Z_C| > 2R \quad ; \quad \text{(Instability)} \tag{21}$$

$$\frac{1}{LC} = \left(\frac{1}{2RC}\right)^2 \quad \Rightarrow \quad |Z_L| = |Z_C| = 2R \quad ; \quad \text{(Marginal stability)} \tag{22}$$

$$\frac{1}{LC} < \left(\frac{1}{2RC}\right)^2 \quad \Rightarrow \quad |Z_L| = |Z_C| < 2R \quad ; \quad \text{(Stability)} \tag{23}$$

5.2. Stability Test for Parallel RLC Low-Pass Filter

This section will present a stability test for a parallel RLC low-pass filter. Three models of the parallel RLC low-pass filter are used to do the damped oscillation noise test. The marginally stable model is designed at cut-off frequency f_0 = 50 kHz taking L = 796 uH, C = 3.18 nF, and R = 250 Ω based on a balanced charge and discharge time condition as shown in Figure 9(b). Figures 9(a) and 9(c) are unconditionally stable (R = 150 Ω), and unstable (R = 500 Ω), respectively. One current source injection and two splitting current sources are used to measure the self-loop functions. Figures 9(d), 9(e), 9(f), 9(g), 9(h) and 9(i) are the measurements of the self-loop functions. Figure 10(a) represents the SPICE simulation results of these models.

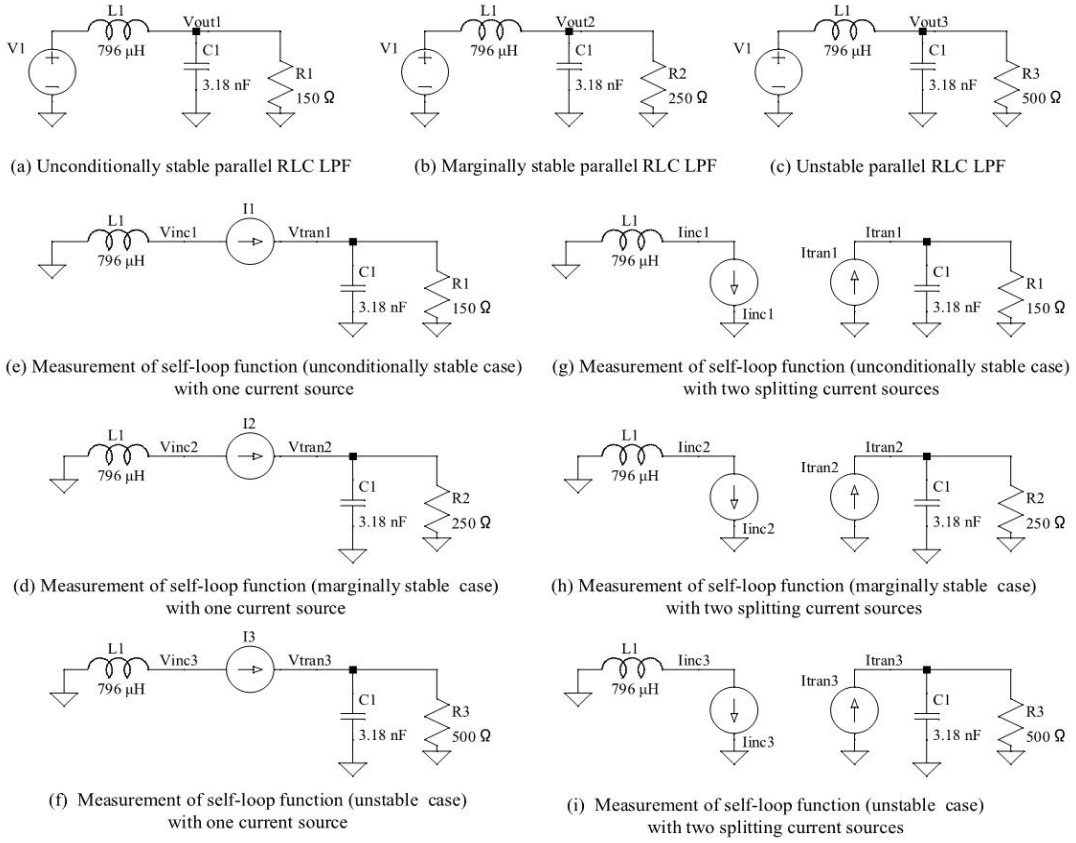

Figure 9. Models of circuits and measurements of self-loop functions for parallel RLC LPF.

The damped oscillation noise (red) occurs in case of the unstable network ($|Z_L| = |Z_C| > 2R$). Our simulation results of self-loop functions show that

- In stable case $|Z_L| = |Z_C| < 2R$, phase is 95.7 degrees at 50 kHz, (phase margin = 84.3 degrees).
- In marginally stable case ($|Z_L| = |Z_C| = 2R$), phase is 104 degrees at 50 kHz, (phase margin = 76 degrees).
- In unstable case ($|Z_L| = |Z_C| > 2R$), phase margin is 116 degrees at 50kHz, (phase margin = 64 degrees).

The simulation results and the values of theoretical calculation are unique.

6. DESIGN OF ACTIVE INDUCTOR FOR RLC LOW-PASS FILTER

6.1. Analysis of General Impedance Converter

In this section, the passive inductor is replaced with a general impedance converter. In integrated circuits, capacitors are much preferred to inductors due to their small size. The general impedance converter acts like an inductor. The behaviour of an inductor can be emulated by an active circuit [9,10]. The general impedance converter is considered as a floating impedance as shown in Figure 11(a). Models of two active RLC low-pass filters are shown Figures 11(b) and 11(c).

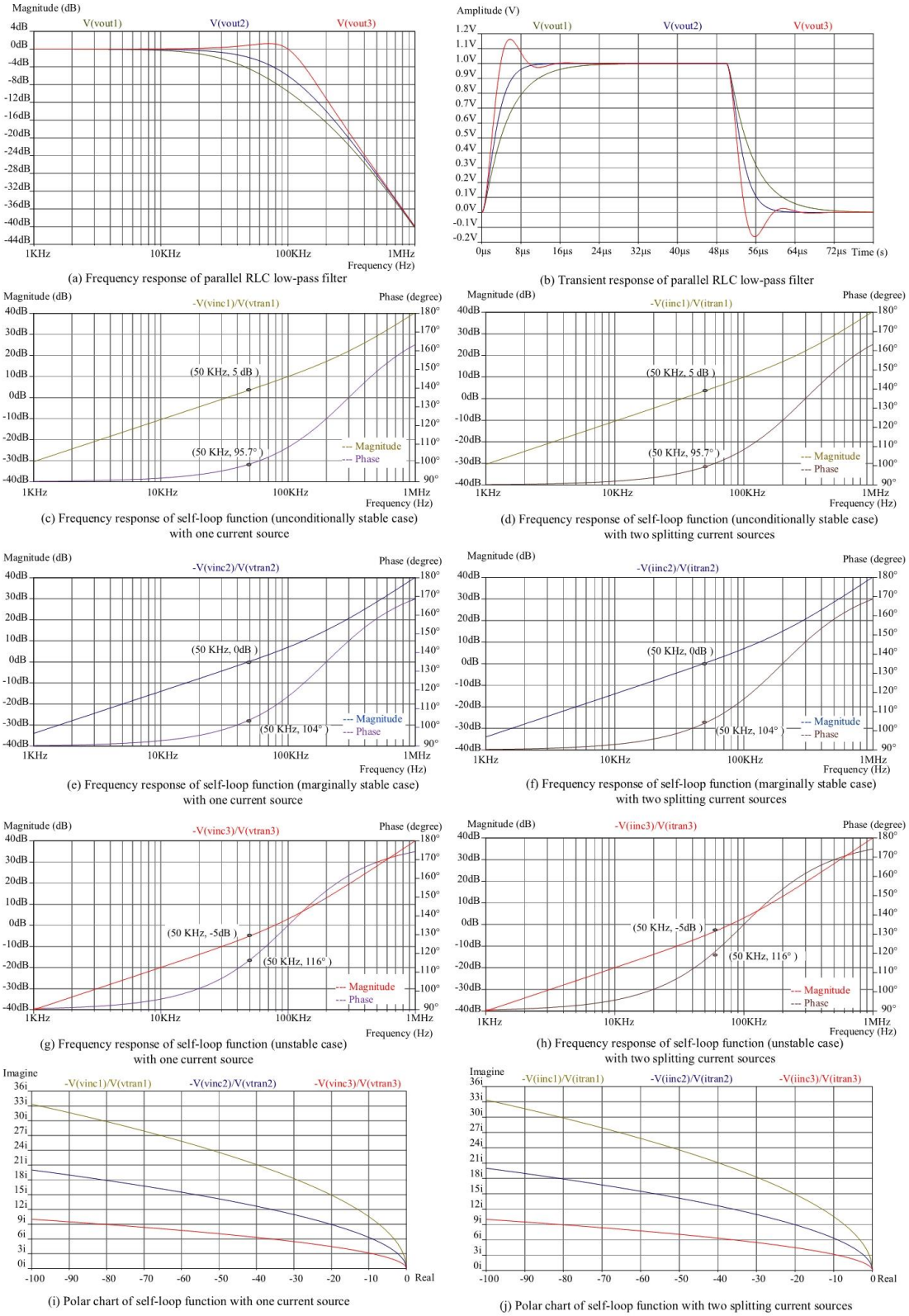

(a) Frequency response of parallel RLC low-pass filter

(b) Transient response of parallel RLC low-pass filter

(c) Frequency response of self-loop function (unconditionally stable case) with one current source

(d) Frequency response of self-loop function (unconditionally stable case) with two splitting current sources

(e) Frequency response of self-loop function (marginally stable case) with one current source

(f) Frequency response of self-loop function (marginally stable case) with two splitting current sources

(g) Frequency response of self-loop function (unstable case) with one current source

(h) Frequency response of self-loop function (unstable case) with two splitting current sources

(i) Polar chart of self-loop function with one current source

(j) Polar chart of self-loop function with two splitting current sources

Figure 10. Frequency response, transient response, polar charts and magnitude-phase plots of self-loop function for serial RLC low-pass filter.

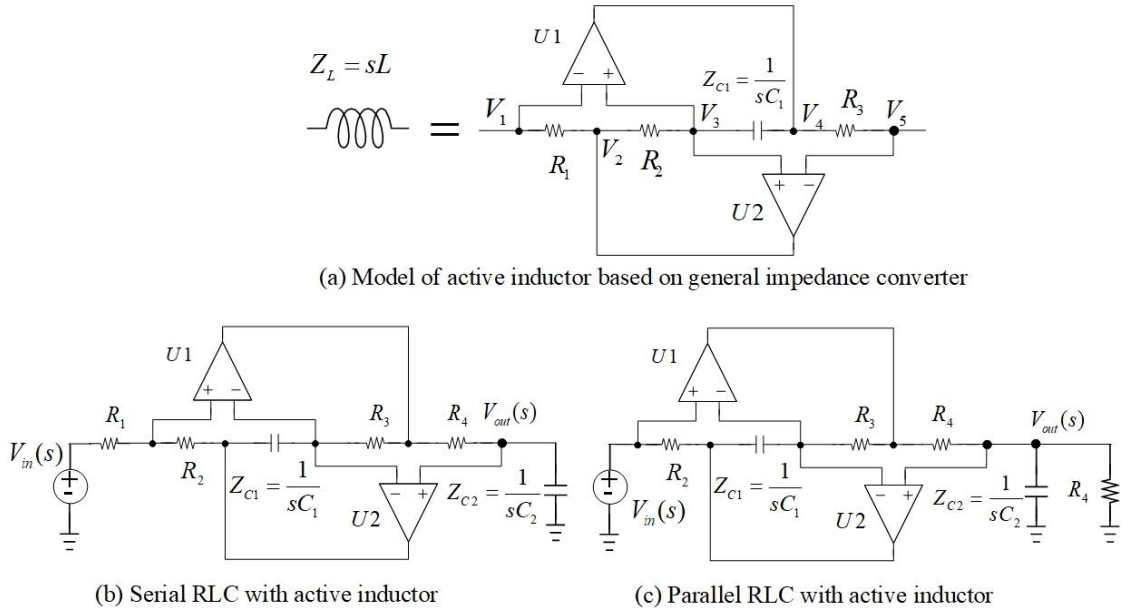

Figure 11. Proposed design of active inductors for RLC low-pass filters.

The feedback loops which are provided by the two op amps force $V_1 - V_3$ and $V_3 - V_5$ to zero.

$$V_1 = V_3 = V_5 \tag{24}$$

Apply the superposition at node V_3, and we get

$$V_3\left(\frac{1}{R_2} + \frac{1}{Z_C}\right) = \frac{V_2}{R_2} + \frac{V_4}{Z_C} \tag{25}$$

The impedance of active inductor is designed as R_1, R_2, R_3, and Z_C chosen properly. From Equations (24) and (25), the value of this inductor is

$$Z_L = \frac{R_2}{R_1}\frac{R_3}{Z_C}Z_{out} = \frac{R_2 R_3}{R_1} sCZ_{out} \tag{26}$$

Here, Z_{out} is the output impedance. This circuit converts a resistor to an inductor. Figure 12 shows the models of the proposed design of the active RLC low-pass filters.

6.2. SPICE Simulations for Active RLC Low Pass Filters

In this section, SPICE simulations are carried out using the ideal operational amplifier with the gain bandwidth (GBW) = 10 MHz and DC value of open loop gain (A(s)) = 100000. Two RLC circuits in Figure 12(a) and 12(b) are designed at the cut-off frequency f_0 = 50 kHz taking C1 = 3.18 nF, L1 = 796 μH, R1 = 1 kΩ, R2 = 250 Ω. In this paper, the 796 μH inductor is replaced with a general impedance converter which includes two op amps and three resistors as well as a capacitor. Figure 12(c) represents the active serial RLC circuit designed with R2 = R3 = 1 kΩ, C2 = 0.1 pF and R4 = 25 kΩ. Figure 12(d) represents the active serial RLC circuit designed with R1 = R3 = 1 kΩ, C2 = 0.1 pF, and R4 = 25 kΩ. The simulation results of the passive and the active RLC low-pass filters are unique as shown in Figures 12(e), 12(f), 12(g), and 12(h).

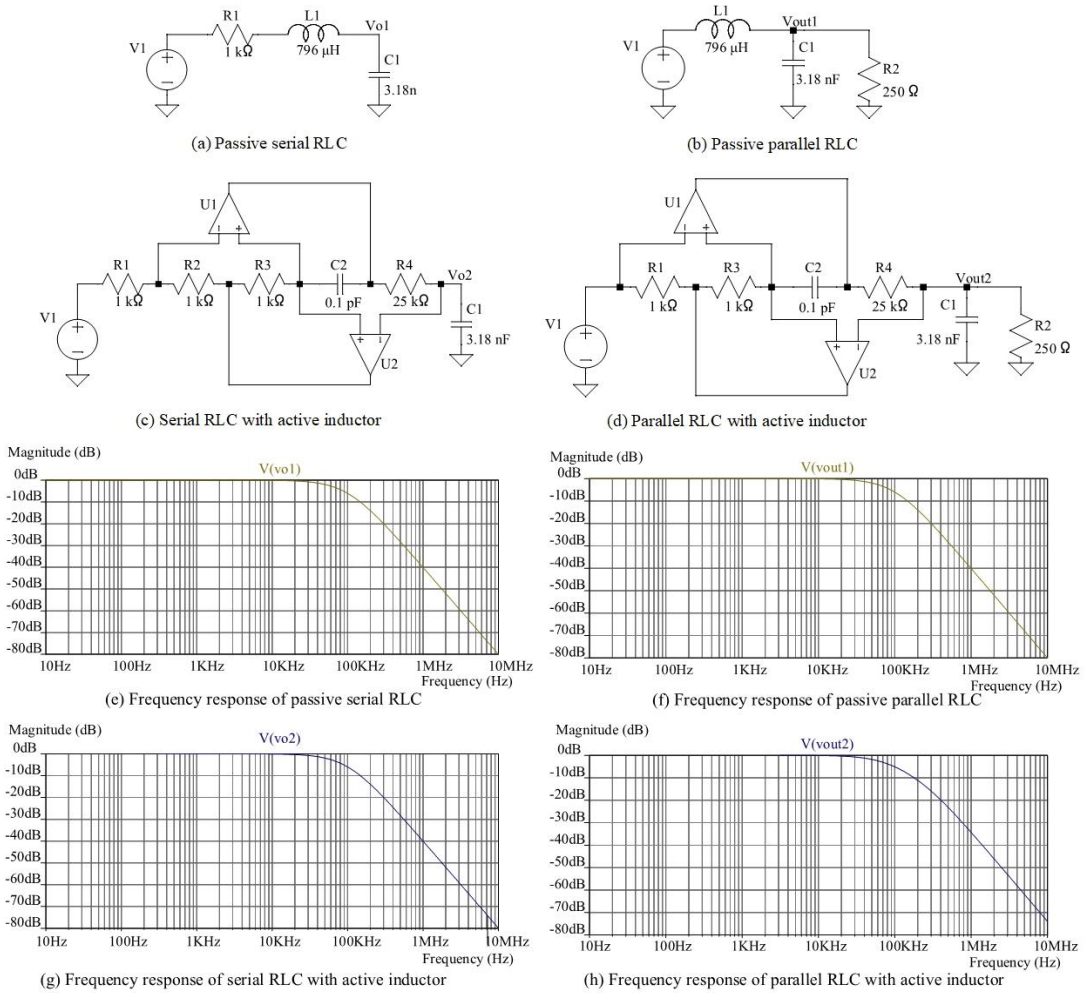

Figure 12. Proposed design and SPICE simulation results of active RLC low-pass filters.

7. DISCUSSION

The performance of a passive RLC low-pass filter is determined by its self-loop function and the step input response. These measurements show how good a second-order low-pass filter is. The self-loop function of a low-pass filter is only important if it gives some useful information about relative stability or if it helps optimize the performance of system. The self-loop function can be directly calculated based on the widened superposition principle. The alternating current conservation technique (voltage injection) can measure the self-loop function of low-pass filters. Compared to the research results with mathematical analysis, the properties of self-loop functions are the same. Moreover, Nyquist theorem shows that the polar plot of self-loop function L(s) must not encircle the point (−1, 0) clockwise as *s* traverses a contour around the critical region clockwise in polar chart [11]. However, Nyquist theorem is only used in theoretical analysis for feedback systems.

8. CONCLUSIONS

This paper describes the approach to do the stability test for RLC low-pass filters. The transfer functions of these filters are second-order denominator complex function. Moreover, the term of "self-loop function" is proposed to define L(s) in a general transfer function. In order to show an

example of how to define the operating region of a RLC low-pass filter, a second-order denominator complex function is analyzed. In overdamped case, the filter will amplify the high order harmonics from the first cut-off angular frequency ω_{cut1} to the second cut-off angular frequency ω_{cut2} of a step input. This causes the unwanted noise which is called ringing or overshoot.

The term of "damped oscillation noise" is proposed to define the ringing. The values of the passive components used in the filter circuit were chosen directly by the stable conditions. The passive inductor is replaced by a general impedance converter. All of the transfer functions were derived based on the widened superposition principle and self-loop functions were measured according to the alternating current conservation technique.

The obtained results were acquired to simulations using SPICE models of the devices, including the model of an ideal operational amplifier. The frequency responses from the proposed active RLC low-pass filters are matched with the passive ones. In this paper not only the results of the mathematical model but also the simulation results of the designed circuits are provided, including the stability test. The simulation results and the values of theoretical calculation of the self-loop function are unique. Furthermore, managing power consumption of circuits and systems is one of the most important challenges for the semiconductor industry [12,13]. Therefore, the damped oscillation noise test can be used to evaluate the stability of a high-order filter.

ACKNOWLEDGEMENTS

Foremost, we would like to express our sincere gratitude to advisor, Prof. Tanimoto (Kitami Institute. of Technology, Japan) for continuing supports.

REFERENCES

[1] H. Kobayashi, N. Kushita, M. Tran, K. Asami, H. San, A. Kuwana "Analog - Mixed-Signal - RF Circuits for Complex Signal Processing", *IEEE 13th International Conference on ASIC* (ASICON 2019) Chongqing, China (Nov, 2019).

[2] M. Tran, C. Huynh, "A Design of RF Front-End for ZigBee Receiver using Low-IF Architecture with Poly-phase Filter for Image Rejection", *M.S. thesis, University of Technology Ho Chi Minh City* – Vietnam (Dec. 2014).

[3] H. Kobayashi, M. Tran, K. Asami, A. Kuwana, H. San, "Complex Signal Processing in Analog, Mixed - Signal Circuits", *Proceedings of International Conference on Technology and Social Science 2019*, Kiryu, Japan (May. 2019).

[4] M. Tran, N. Kushita, A. Kuwana, H. Kobayashi "Flat Pass-Band Method with Two RC Band-Stop Filters for 4-Stage Passive RC Quadratic Filter in Low-IF Receiver Systems", *IEEE 13th International Conference on ASIC* (ASICON 2019) Chongqing, China (Nov. 2019).

[5] M. Tran, Y. Sun, N. Oiwa, Y. Kobori, A. Kuwana, H. Kobayashi, "Mathematical Analysis and Design of Parallel RLC Network in Step-down Switching Power Conversion System", *Proceedings of International Conference on Technology and Social Science* (ICTSS 2019) Kiryu, Japan (May. 2019).

[6] M. Tran, "Damped Oscillation Noise Test for Feedback Circuit Based on Comparison Measurement Technique", *73rd System LSI Joint Seminar, Tokyo Institute of Technology*, Tokyo, Japan (Oct. 2019).

[7] R. Middlebrook, "Measurement of Loop Gain in Feedback Systems", *Int. J. Electronics*, Vol 38, No. 4, pp. 485-512, (1975).

[8] M. Tran, Y. Sun, Y. Kobori, A. Kuwana, H. Kobayashi, "Overshoot Cancelation Based on Balanced Charge-Discharge Time Condition for Buck Converter in Mobile Applications", *IEEE 13th International Conference on ASIC* (ASICON 2019) Chongqing, China (Nov, 2019).

[9] A. Sedra, K. Smith (2010) *Microelectronic Circuits* 6th ed. Oxford University Press, New York.

[10] R. Schaumann, M. Valkenberg, (2001) *Design of Analog Filters*, Oxford University Press.

[11] B. Razavi, (2016) *Design of Analog CMOS Integrated Circuits*, 2nd Edition McGraw-Hill.
[12] M. Tran, N. Miki, Y. Sun, Y. Kobori, H. Kobayashi, "EMI Reduction and Output Ripple Improvement of Switching DC-DC Converters with Linear Swept Frequency Modulation", *IEEE 14th International Conference on Solid-State and Integrated Circuit Technology*, Qingdao, China (Nov. 2018).
[13] J. Wang, G. Adhikari, N. Tsukiji, M. Hirano, H. Kobayashi, K. Kurihara, A. Nagahama, I. Noda, K. Yoshii, "Equivalence Between Nyquist and Routh-Hurwitz Stability Criteria for Operational Amplifier Design", *IEEE International Symposium on Intelligent Signal Processing and Communication Systems* (ISPACS), Xiamen, China (Nov. 2017).

APPENDIX

A.1. Second-order denominator complex function

From Equation (8), the transfer function is rewritten as

$$H(s=j\omega)=\frac{1}{as^2+bs+c}=\frac{\frac{4a}{b^2}}{\left(1+j\frac{2a}{b}\omega\right)^2+\left(\frac{2a}{b}\right)^2\left[\frac{c}{a}-\left(\frac{b}{2a}\right)^2\right]} \tag{27}$$

The magnitude-angular form of transfer function is

$$|H(j\omega)|=\frac{4a}{b^2}\frac{1}{\sqrt{\left(\frac{4a}{b}\omega\right)^2+\left(1-\left(\frac{2a}{b}\omega\right)^2+\left(\frac{2a}{b}\right)^2\left[\frac{c}{a}-\left(\frac{b}{2a}\right)^2\right]\right)^2}};\ \angle H(j\omega)=\arctan\left(\frac{-\frac{4a}{b}\omega}{1-\left(\frac{2a}{b}\omega\right)^2+\left(\frac{2a}{b}\right)^2\left[\frac{c}{a}-\left(\frac{b}{2a}\right)^2\right]}\right) \tag{28}$$

In critically damped case $\frac{c}{a}=\left(\frac{b}{2a}\right)^2$, the magnitude-angular form of transfer function is

$$|H(j\omega)|=\frac{4a}{b^2}\frac{1}{\sqrt{\left(\frac{4a}{b}\omega\right)^2+\left(1-\left(\frac{2a}{b}\omega\right)^2\right)^2}};\ \angle H(j\omega)=\arctan\left(\frac{-\frac{4a}{b}\omega}{1-\left(\frac{2a}{b}\omega\right)^2}\right) \tag{29}$$

At the cut-off angular frequency $\omega_{cut}=\frac{b}{2a}$, the values of magnitude and angular are

$$|H(j\omega)|=\frac{2a}{b^2};\ \angle H(j\omega)=\arctan(-\infty)=-\frac{\pi}{2} \tag{30}$$

A.2. Self-loop function of second-order denominator complex function

From Equation (11), the self-loop function is rewritten as

$$L(j\omega)=j\frac{4a}{b}\omega+\left(j\frac{2a}{b}\omega\right)^2+\left(\frac{2a}{b}\right)^2\left[\frac{c}{a}-\left(\frac{b}{2a}\right)^2\right] \tag{31}$$

The magnitude-angular and the real-imagine parts of self-loop function are

$$|L(j\omega)| = \sqrt{\left(\frac{4a}{b}\omega\right)^2 + \left(\left(\frac{2a}{b}\right)^2\left[\frac{c}{a} - \left(\frac{b}{2a}\right)^2\right] - \left(\frac{2a}{b}\omega\right)^2\right)^2};\ \angle L(j\omega) = \arctan\left(\frac{\frac{4a}{b}\omega}{\left(\frac{2a}{b}\right)^2\left[\frac{c}{a} - \left(\frac{b}{2a}\right)^2\right] - \left(\frac{2a}{b}\omega\right)^2}\right) \tag{32}$$

$$\mathrm{Re}\{L(j\omega)\} = \left(\frac{2a}{b}\right)^2\left[\frac{c}{a} - \left(\frac{b}{2a}\right)^2\right] - \left(\frac{2a}{b}\omega\right)^2;\ \mathrm{Im}\{L(j\omega)\} = \frac{4a}{b}\omega$$

In critically damped case $\frac{c}{a} = \left(\frac{b}{2a}\right)^2$, the self-loop function is

$$L(j\omega) = j\frac{4a}{b}\omega\left(1 + j\frac{a}{b}\omega\right) = \sqrt{\left(\frac{4a}{b}\omega\right)^2 + \left(\frac{2a}{b}\omega\right)^4}\, e^{j\arctan\left(\frac{2}{-\left(\frac{2a}{b}\omega\right)}\right)} \tag{33}$$

At the angular frequency $\omega = \frac{b}{a}$, the magnitude-angular and the real-imagine values are

$$|L(j\omega)| = 4\sqrt{2};\ \ \angle L(\omega) = \arctan(-1) = -45^o;\ \mathrm{Re}\{L(j\omega)\} = -4;\ \mathrm{Im}\{L(j\omega)\} = 4 \tag{34}$$

Do the same work, at the angular frequency $\omega_{cut} = \frac{b}{2a}$, we have

$$\begin{aligned} &|L(j\omega)| = \sqrt{5};\ \angle L(j\omega) = \arctan(-2) = -63.4^o \\ &\mathrm{Re}\{L(j\omega)\} = -1;\ \ \mathrm{Im}\{L(j\omega)\} = 2 \end{aligned} \tag{35}$$

At unity gain of the self-loop function, we have

$$|L(\omega_u)| = 1 \Rightarrow \left|\frac{4a}{b}\omega_u\sqrt{1 + \left(\frac{a}{b}\omega_u\right)^2}\right| = 1 \tag{36}$$

Solving Equation (43), the angular frequency ω_u at unity gain is

$$\omega_u = \frac{b}{2a}\sqrt{\sqrt{5} - 2} \qquad \Rightarrow \qquad \omega_{cut} = \frac{\omega_u}{\sqrt{\sqrt{5} - 2}} \tag{37}$$

Here, the cut-off angular frequency is $\omega_{cut} = \frac{b}{2a}$.

At unity gain angular frequency $\omega_u = \frac{b}{2a}\sqrt{\sqrt{5} - 2}$, the magnitude-angular and the real-imagine values are

$$|L(j\omega)|=1;\ \angle L(j\omega)=\arctan\left(\frac{-2}{\sqrt{\sqrt{5}-2}}\right)=-76.35^{o}$$
$$\mathrm{Re}\{L(j\omega)\}=2-\sqrt{5};\ \ \mathrm{Im}\{L(j\omega)\}=2\sqrt{\sqrt{5}-2} \tag{38}$$

In underdamped case $\frac{c}{a}<\left(\frac{b}{2a}\right)^2$, the self-loop function is

$$L(j\omega)=j\frac{4a}{b}\omega-\left(j\frac{2a}{b}\omega\right)^2-\left|\left(\frac{2a}{b}\right)^2\left[\frac{c}{a}-\left(\frac{b}{2a}\right)^2\right]\right| \tag{39}$$

Here, the magnitude-angular and the real-imagine parts of self-loop function are

$$|L(j\omega)|=\sqrt{\left(\frac{4a}{b}\omega\right)^2+\left(-\left|\left(\frac{2a}{b}\right)^2\left[\frac{c}{a}-\left(\frac{b}{2a}\right)^2\right]\right|-\left(\frac{2a}{b}\omega\right)^2\right)^2};\ \angle L(j\omega)=\arctan\left(\frac{\frac{4a}{b}\omega}{-\left|\left(\frac{2a}{b}\right)^2\left[\frac{c}{a}-\left(\frac{b}{2a}\right)^2\right]\right|-\left(\frac{2a}{b}\omega\right)^2}\right) \tag{40}$$
$$\mathrm{Re}\{L(j\omega)\}=-\left|\left(\frac{2a}{b}\right)^2\left[\frac{c}{a}-\left(\frac{b}{2a}\right)^2\right]\right|-\left(\frac{2a}{b}\omega\right)^2;\mathrm{Im}\{L(j\omega)\}=\frac{4a}{b}\omega$$

At the angular frequency $\omega=\frac{b}{a}$, we have

$$|L(j\omega)|=\sqrt{(4)^2+\left(-\left|\left(\frac{2a}{b}\right)^2\left[\frac{c}{a}-\left(\frac{b}{2a}\right)^2\right]\right|-(4)^2\right)^2}>4\sqrt{2};\ \angle L(j\omega)=\arctan\left(\frac{4}{-\left|\left(\frac{2a}{b}\right)^2\left[\frac{c}{a}-\left(\frac{b}{2a}\right)^2\right]\right|-4}\right)<\arctan(-1)=-45^{o} \tag{41}$$
$$\mathrm{Re}\{L(j\omega)\}=4-\left|\left(\frac{2a}{b}\right)^2\left[\frac{c}{a}-\left(\frac{b}{2a}\right)^2\right]\right|<4;\quad \mathrm{Im}\{L(j\omega)\}=4$$

At the angular frequency $\omega_{cut}=\frac{b}{2a}$, we have

$$|L(j\omega)|=\sqrt{4+\left(-\left|\left(\frac{2a}{b}\right)^2\left[\frac{c}{a}-\left(\frac{b}{2a}\right)^2\right]\right|-1\right)^2}>\sqrt{5};\ \angle L(j\omega)=\arctan\left(\frac{2}{-\left|\left(\frac{2a}{b}\right)^2\left[\frac{c}{a}-\left(\frac{b}{2a}\right)^2\right]\right|-1}\right)<\arctan(-2)=-63.4^{o} \tag{42}$$
$$\mathrm{Re}\{L(j\omega)\}=-\left|\left(\frac{2a}{b}\right)^2\left[\frac{c}{a}-\left(\frac{b}{2a}\right)^2\right]\right|-4<-4;\ \mathrm{Im}\{L(j\omega)\}=4$$

Then, at unity gain angular frequency $\omega_u=\frac{b}{2a}\sqrt{\sqrt{5}-2}$, we have

$$|L(j\omega)|=\sqrt{2(\sqrt{5}-2)+\left(-\left|\left(\frac{2a}{b}\right)^2\left[\frac{c}{a}-\left(\frac{b}{2a}\right)^2\right]\right|+2-\sqrt{5}\right)^2}>1;\ \angle L(j\omega)=\arctan\left(\frac{2\sqrt{\sqrt{5}-2}}{-\left|\left(\frac{2a}{b}\right)^2\left[\frac{c}{a}-\left(\frac{b}{2a}\right)^2\right]\right|-(\sqrt{5}-2)}\right)<\arctan\left(\frac{-2}{\sqrt{\sqrt{5}-2}}\right)=-76.35^{o} \tag{43}$$

$$\mathrm{Re}\{L(j\omega)\} = -\left|\left(\frac{2a}{b}\right)^2\left[\frac{c}{a}-\left(\frac{b}{2a}\right)^2\right]\right| + 2 - \sqrt{5} > 2 - \sqrt{5}; \mathrm{Im}\{L(j\omega)\} = 2\sqrt{\sqrt{5}-2}$$

In overdamped case $\frac{c}{a} > \left(\frac{b}{2a}\right)^2$, the self-loop function is

$$L(j\omega) = j\frac{4a}{b}\omega - \left(j\frac{2a}{b}\omega\right)^2 + \left|\left(\frac{2a}{b}\right)^2\left[\frac{c}{a}-\left(\frac{b}{2a}\right)^2\right]\right| \tag{44}$$

Here, the magnitude-angular and the real-imagine parts of self-loop function are

$$|L(j\omega)| = \sqrt{\left(\frac{4a}{b}\omega\right)^2 + \left(\left|\left(\frac{2a}{b}\right)^2\left[\frac{c}{a}-\left(\frac{b}{2a}\right)^2\right]\right| - \left(\frac{2a}{b}\omega\right)^2\right)^2}; \angle L(j\omega) = \arctan\left(\frac{\frac{4a}{b}\omega}{\left|\left(\frac{2a}{b}\right)^2\left[\frac{c}{a}-\left(\frac{b}{2a}\right)^2\right]\right| - \left(\frac{2a}{b}\omega\right)^2}\right) \tag{45}$$

$$\mathrm{Re}\{L(j\omega)\} = \left|\left(\frac{2a}{b}\right)^2\left[\frac{c}{a}-\left(\frac{b}{2a}\right)^2\right]\right| - \left(\frac{2a}{b}\omega\right)^2; \mathrm{Im}\{L(j\omega)\} = \frac{4a}{b}\omega$$

At the angular frequency $\omega = \frac{b}{a}$, the magnitude-angular and the real-imagine values are

$$|L(j\omega)| = \sqrt{(4)^2 + \left(\left|\left(\frac{2a}{b}\right)^2\left[\frac{c}{a}-\left(\frac{b}{2a}\right)^2\right]\right| - (4)^2\right)^2} < 4\sqrt{2}; \angle L(j\omega) = \arctan\left(\frac{4}{\left|\left(\frac{2a}{b}\right)^2\left[\frac{c}{a}-\left(\frac{b}{2a}\right)^2\right]\right| - 4}\right) > \arctan(-1) = -45^o \tag{46}$$

$$\mathrm{Re}\{L(j\omega)\} = \left|\left(\frac{2a}{b}\right)^2\left[\frac{c}{a}-\left(\frac{b}{2a}\right)^2\right]\right| - 4 > -4; \ \mathrm{Im}\{L(j\omega)\} = 4$$

Then, at the angular frequency $\omega_{cut} = \frac{b}{2a}$, we have

$$|L(j\omega)| = \sqrt{4 + \left(\left|\left(\frac{2a}{b}\right)^2\left[\frac{c}{a}-\left(\frac{b}{2a}\right)^2\right]\right| - 1\right)^2} < \sqrt{5}; \angle L(j\omega) = \arctan\left(\frac{2}{\left|\left(\frac{2a}{b}\right)^2\left[\frac{c}{a}-\left(\frac{b}{2a}\right)^2\right]\right| - 1}\right) > \arctan(-2) = -63.4^o \tag{47}$$

$$\mathrm{Re}\{L(j\omega)\} = 4 + \left|\left(\frac{2a}{b}\right)^2\left[\frac{c}{a}-\left(\frac{b}{2a}\right)^2\right]\right| > 4; \quad \mathrm{Im}\{L(j\omega)\} = 4$$

At unity gain angular frequency $\omega_u = \frac{b}{2a}\sqrt{\sqrt{5}-2}$, we have

$$|L(j\omega)| = \sqrt{2(\sqrt{5}-2) + \left(\left|\left(\frac{2a}{b}\right)^2\left[\frac{c}{a}-\left(\frac{b}{2a}\right)^2\right]\right| + 2 - \sqrt{5}\right)^2} < 1; \angle L(j\omega) = \arctan\left(\frac{2\sqrt{\sqrt{5}-2}}{\left|\left(\frac{2a}{b}\right)^2\left[\frac{c}{a}-\left(\frac{b}{2a}\right)^2\right]\right| - (\sqrt{5}-2)}\right) > \arctan\left(\frac{-2}{\sqrt{\sqrt{5}-2}}\right) = -76.35^o \tag{48}$$

$$\mathrm{Re}\{L(j\omega)\} = \left|\left(\frac{2a}{b}\right)^2\left[\frac{c}{a}-\left(\frac{b}{2a}\right)^2\right]\right| - 1 > -1; \ \mathrm{Im}\{L(j\omega)\} = 2$$

AUTHORS

Minh Tri Tran received the B.S. and M.S. degree from the University of Technical Education Ho Chi Minh City (HCMUTE) – Vietnam, and University of Technology Ho Chi Minh City (HCMUT) – Vietnam, in 2011, and 2014, respectively, all in Electrical and Electronic Engineering. He joined the Division of Electronics and Informatics, Gunma University, Japan in 2018, where he is presently working toward the Ph.D. degree in Electrical and Electronic Engineering. His research interests include modelling, analysis, and test of damped oscillation noise and radio-frequency radiation noise in communication systems.

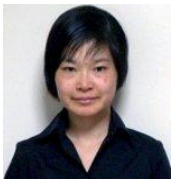

Anna Kuwana received the B.S. and M.S. degrees in information science from Ochanomizu University in 2006 and 2007 respectively. She joined Ochanomizu University as a technical staff, and received the Ph.D. degree by thesis only in 2011. She joined Gunma University and presently is an assistant professor in Division of Electronics and Informatics there. Her research interests include computational fluid dynamics.

Haruo Kobayashi received the B.S. and M.S. degrees in information physics from University of Tokyo in 1980 and 1982 respectively, the M.S. degree in electrical engineering from University of California, Los Angeles (UCLA) in 1989, and the Ph. D. degree in electrical engineering from Waseda University in 1995. In 1997, he joined Gunma University and presently is a Professor in Division of Electronics and Informatics there. His research interests include mixed-signal integrated circuit design & testing, and signal processing algorithms.